water

MDPI

Article

Characterization and Disinfection by Product Formation of Dissolved Organic Matter in Anaerobic–Anoxic–Oxic Membrane Bioreactor (AAO-MBR) Process

Xueli Ren [1,†], Feng Wang [2,†], Yajing Zhang [1], Jiali Wang [3] and Hengfeng Miao [1,4,5,*]

[1] School of Environmental and Civil Engineering, Jiangnan University, Wuxi 214122, China; renxueli666@163.com (X.R.); 8202202019@jiangnan.edu.cn (Y.Z.)
[2] Wuxi Ecological Environment Monitoring Center, Wuxi 214122, China; wolfwxh@aliyun.com
[3] Yixing Ecological Environment Monitoring Station, Wuxi 214122, China
[4] Jiangsu Key Laboratory of Anaerobic Biotechnology, Jiangnan University, Wuxi 214122, China
[5] Jiangsu Collaborative Innovation Center of Technology and Material of Water Treatment, Suzhou 215009, China
* Correspondence: hfmiao2008@163.com
† These authors contributed equally to this work.

Abstract: In the process of sewage treatment, the characteristics of dissolved organic matter (DOM) are always changed during chemical and biological processes, affecting the generation of disinfection by-products (DBPs) compositions at the following disinfection stage. The present study systematically investigated the effect of DOM characterization on C- and N-DBPs formation at AAO-MBR reactor when treating wastewater. The results showed that the AAO-MBR treatment process could efficiently eliminate dissolved organic carbon (DOC) and ammonium nitrogen (NH_4^+-N) from wastewater with an elimination rate of 89% and 98%, respectively. Most of the precursors (i.e., 56.8% C-DBPs and 78.1% N-DBPs) were removed at the MBR unit, while AGC and AAO units promoted the formation of DBPs precursors. More specifically, soluble microbial products (SMPs) and humus acid were increased, which led to improved C- and N-DBPs via aerated grit chamber (AGC) treatment. At the AAO treatment unit, the content of low MW hydrophobic SMPs, humus acid, and polysaccharides was increased, indicating low MW and HPO fractions dominating the C- and N-DBPs. MBR treatment improved C-DBPs in high MW and HPO fractions and N-DBPs in low MW and HPO fractions, which is explained by higher MW hydrophobic SMPs and humus acids, compared to the AAO unit. The present study provided deep insight into the linkage of DOM characteristics and C- and N-DBPs formation at each treatment unit during the AAO-MBR process.

Keywords: dissolved organic matter (DOM); disinfection by-products (DBPs); AAO-MBR process; molecular weight (MW); soluble microbial products (SMPs)

check for updates

Citation: Ren, X.; Wang, F.; Zhang, Y.; Wang, J.; Miao, H. Characterization and Disinfection by Product Formation of Dissolved Organic Matter in Anaerobic–Anoxic–Oxic Membrane Bioreactor (AAO-MBR) Process. *Water* **2023**, *15*, 1076. https://doi.org/10.3390/w15061076

Academic Editor: Zacharias Frontistis

Received: 3 February 2023
Revised: 7 March 2023
Accepted: 8 March 2023
Published: 10 March 2023

Copyright: © 2023 by the authors. Licensee MDPI, Basel, Switzerland. This article is an open access article distributed under the terms and conditions of the Creative Commons Attribution (CC BY) license (https://creativecommons.org/licenses/by/4.0/).

1. Introduction

Wastewater reuse is an effective way to solve the water shortage problem [1–3]. To ensure safety of reclaimed water, disinfection is an indispensable process to inactivate bacteria, viruses, and other microorganisms [4]. During the disinfection process, disinfectants can react with different types of dissolved organic matter (DOM) in wastewater, leading to the formation of disinfection by-products (DBPs) [5]. Until now, more than 800 DBPs have been detected at chlorine disinfection, including trihalomethanes (THMs) and haloacetic acids (HAAs) [6]. THMs, HAAs, and other halogenated DBPs have genotoxic, mutagenic, and carcinogenic, threatening human health [7].

DOM contains polysaccharides, proteins, and humus with groups of amino, carboxyl, ester, hydroxyl, ketone, and phenol [8]. Dissolved organic carbon (DOC) is the precursor of carbon-containing DBPs (C-DBPs), such as THMs and HAAs, whereas dissolved organic nitrogen (DON) is the precursor of nitrogen-containing DBPs (N-DBPs) [9]. Compared

with N-DBPs, the concentration of C-DBPs is higher (μg L^{-1}), but the genetic toxicity is lower [10]. As a result, the study in the classification of DBPs and their precursors is more significant than that of the total DBPs. The DBP precursors could be characterized by three-dimensional excitation and emission matrix (3D-EEM), specific ultraviolet absorbance (SUVA), Fourier transform infrared (FT-IR), nuclear magnetic resonance (NMR), and high performance size exclusion chromatography (HPSEC) with UV-detection [11,12]. Many studies have reported the characterization of DBP precursors by SUVA and 3D-EEM [13]. The functional groups in the organic matter were characterized by FT-IR and NMR.

The hydrophobicity and molecular weight (MW) of DOM are considered as main factors influencing DBPs formation. According to MW, three types of DOM were divided, including large MW (>10 kDa), medium MW (1–10 kDa, such as humic/fulvic acids), and low MW (<1 kDa, such as carbohydrates and amino acids) [14]. The hydrophobicity and electron density of DOM are influenced by different functional groups, which affect the apparent reactivity to chlorine and the following DBPs formation [15]. DOM also can be divided into different fractions, including the hydrophilic fraction (HPI), the hydrophobic fraction (HPO), and the transphilic fraction (TPI) [16]. HPO usually contains high MW unsaturated functional groups, which are derived from raw wastewater [6]. Conversely, HPI has traditionally low MW amino acids and soluble microbial products (SMPs), which are considered metabolites of microorganisms [17]. It was reported that SMPs composed of protein, polysaccharides, humic acid, and so on. Moreover, SMPs can react with chlorine to generate DBPs [18]. Compared with HPI, HPO shows a higher possibility for N-DBPs formation due to containing more active DON in hydrophilic neutral components [6]. Previous reports found that humic acid is the main DBP precursor that can produce aldehyde and chromic acid [19].

To avoid DBPs generation in reclaimed water, controlling its precursor plays an important role. To this end, DOM removal in the process of wastewater treatment is the main measure currently adopted. It was reported that DOM in wastewater could be removed by biological treatment technology with high efficiency, low cost, and environmental friendliness [20]. However, microorganisms produce refractory SMP-like substances by metabolism with organics in the biological treatment process, which is considered the main DBP precursor [21]. To improve DOM removal, the MBR unit is usually used in municipal sewage treatment plants. Despite obtaining a promising effluent quality, the halogenated DBP in the MBR effluent was higher than that of the AAO effluent, especially trichloromethane (TCM) [22]. In the biological treatment process, a low MW fraction is easy to degrade, but a high MW fraction is more difficult to biodegradable [23]. The hydrophobicity and MW of DOM were significantly affected by different treatment processes [14]. The metabolism of organic matter in the wastewater treatment process would change the biological properties of DOM [23]. Han et al. [24] reported that after biological treatment, the MW > 100 kDa accounted for 52%, while the MW < 10 kDa was less than 14% [25]. In the biological treatment process, the DOM with MW less than 500 kDa could be removed with high efficiency, while high MW fractions (e.g., refractory humic-like constitutions and SMPs) were accumulated. Regarding the DBPs, their types and biotoxicity were extensively investigated, but the changes in DOM characteristics on its formation at the AAO-MBR reactor were not fully revealed.

The present study aimed to investigate the changes in DOM characteristics in the AAO-MBR process with aspects of its MW and fractions (HPI, HPO, and TPI) and to reveal the relationship between its characteristics and the formation of C- and N-DBPs in each processing unit.

2. Materials and Methods

2.1. Wastewater Samples

Wastewater was collected from a municipal wastewater treatment plant (WWTP) in Wuxi, China. The treatment processes in WWTP were as follows: AGC process, AAO treatment process, and MBR process. The sampling points are displayed in Figure 1. In

AAO, hydraulic retention time (HRT) was 10.73 h, solid retention time (SRT) was 20.5 d, and the aeration rate was 350 m^3/min in the aerobic tank. MBR unit was equipped with a 0.1 μm PVDF hollow-fiber membrane module, and SRT was 40 d. The aeration rate was 450 m^3 min^{-1}. After sampling, wastewater samples were immediately filtered through a membrane filter (pore size 0.45 μm) to remove particles before water quality analysis.

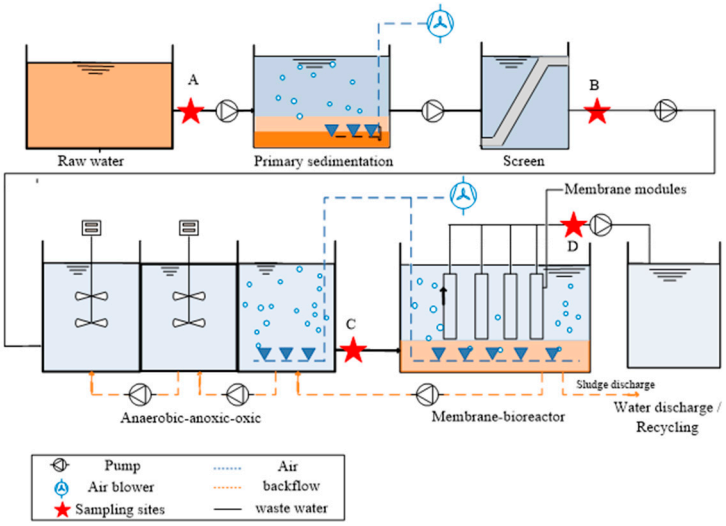

Figure 1. Flowchart of treatment process in the WWTP and sampling scheme ((**A**) Influent; (**B**) AGC effluent; (**C**) AAO effluent; (**D**) MBR effluent).

DOC, dissolved total nitrogen (DTN), ammonium nitrogen (NH_4^+-N), nitrate (NO_3-N), nitrite (NO_2-N), and UV_{254} (UV absorbance at 254 nm) were measured within 24 h. The stored water samples (at 4 °C) were further analyzed, characterized, separated, and chlorinated within 3 days.

2.2. Analytical Methods

Water quality parameters include DOC, DTN, NH_4^+-N, NO_3-N, NO_2-N, UV_{254}, and pH. DOC and DTN were determined with a total organic carbon analyzer (TOC-VCPH, Shimadzu, Kyoto, Japan). DON was calculated by the formula: $DON = DTN - (NH_4^+\text{-}N) - (NO_3\text{-}N) - (NO_2\text{-}N)$. UV_{254} was determined with a spectrophotometer (HACH DR/2000, Loveland, CO, USA). SUVA (Specific UV_{254} absorbance) was calculated as the ratio of UV_{254} to DOC in units of L $(mg{\cdot}m)^{-1}$.

Independent sample t-tests were used to determine whether there were significant differences with SPSS software (IBM SPSS Statistics 19).

2.3. Characterization Methods

2.3.1. Three-Dimensional EEM and FRI Analyses

DOM was analyzed by luminescence spectrometry (F-7000 FL spectrophotometer, Hitachi, Tokyo, Japan). Before 3D-EEM analysis, the DOC of samples was diluted to 3 mg L^{-1}. Three-dimensional EEM spectra were collected with corresponding scanning emission spectra from 250 nm to 550 nm at 5 nm increments by varying the excitation wavelength from 200 nm to 400 nm at 5 nm sampling intervals. Ex and Em slits were maintained at 5 nm, and the scan rate was set at 2400 nm min^{-1}. Deionized water was set as the blank control. All analyses were made in triplicate. Three-dimensional EEM data were analyzed with the software origin 2021.

Fluorescence regional integration (FRI) method was applied to analyze EEM spectra quantitatively [26]. All spectra were normalized by the Raman area [27], and deionized

water was set as the blank control. Fluorescence intensity in one region was accumulated using Formula (1), as shown below.

$$\varphi_{i,n} = MF_i \int_{ex}^{0} \int_{em}^{0} I(\lambda_{ex}\lambda_{em}) d\lambda_{ex}\lambda_{em} \quad (1)$$

$$P_{i,n} = \frac{\varphi_{i,n}}{\varphi_{T,n}} \times 100\% \quad (2)$$

where $\varphi_{i,n}$ is the normalized EEM volume at region i, which represents the cumulative fluorescence response of DOM with similar properties at each region; λ_{ex} is the excitation wavelength interval (taken as 5 nm), λ_{em} is the emission wavelength interval (taken as 5 nm), and I($\lambda_{ex}\lambda_{em}$) is the fluorescence intensity at each excitation-emission wavelength pair; *MF(i)* is a multiplication factor applied to account for the secondary or tertiary responses at longer wavelengths and is equal to the inverse of the fractional projected excitation–emission area; $P_{i,n}$ is the percent of fluorescence response. *MF(i)* was calculated using Formula (3).

$$MF(i) = \frac{Total\ spectr\ aarea}{Specific\ region\ area(i)} \quad (3)$$

According to the FRI method, the EEM spectrum is divided into four regions: region I ($E_{X200\sim250}/E_{M200\sim380}$, protein, in particular, a lysine protein, tryptophan protein or a lysine analog, and tryptophan analogs); region II ($E_{X200\sim250}/E_{M380\sim500}$, fulvic acid or fulvic acid analogs); region III ($E_{X250\sim280}/E_{M200\sim380}$, microbial metabolites, and other biopolymers); region IV ($E_{X250\sim400}/E_{M380\sim500}$, humus or humic acid analogs and other substances) [28].

2.3.2. FT-IR and ^{1}H-NMR Analyses

Fourier transform infrared (FT-IR) was measured by FT-IR spectroscopy (IRTracer-100, Shimadzu, Japan). Before FT-IR analysis, water samples were freeze-dried according to the following procedure. First, 100 mL water samples were taken into the surface of the dish and wrapped with plastic wrap with 8 to 10 holes, and then were placed in a −80 °C refrigerator for 24 h. Next, the frozen samples were freeze-dried by a freeze dryer, and about 2 mg of solid powder was obtained after 24 h. Finally, the solid powder was analyzed by FT-IR spectroscopy. Setting parameters of FT-IR: scan from 4000 to 400 cm^{-1} at an interval of 1.0 cm^{-1} [29].

^{1}H-NMR analysis was conducted with a Bruker NMR spectrometer (Avance III 400 MHz, Basel, Switzerland). Approximately 1 mg of freeze-dried sample was suspended in a 2.0 mL microcentrifuge tube with 1.0 mL deuterium oxide. A few drops of 10% NaOH were added to the mixture to enhance the solubility of the organic matter. After centrifugation at 9500 *g* and 25 ± 2 °C, the supernatant of the sample was collected for NMR analysis with the SGI O_2 R5000 workstation and the Bruker XWinNMRv2.1 software [30].

General assignments for the four major regions of the proton spectra were as follows: I: δ_H = 0.6–1.8, protons on methyl and methylene carbons directly bonded to other carbons (aliphatic protons, H–C); II: δ_H = 1.8–2.6 and δ_H = 2.8–3.2, protons on methyl and methylene carbons alpha to aromatic rings, carboxyl, and carbonyl groups (H–C–C=); III: δ_H = 3.2–4.1, protons on methyl, methylene, or methyne carbons directly bonded to oxygen or nitrogen, including carbohydrate and amino acid protons (H–C–O); IV: 6.0–8.5, protons attached to unsaturated carbons and aromatic protons [31].

2.3.3. Molecular Weight (MW) Distribution

Wastewater samples were separated by 400 mL ultrafiltration units (Millipore, Burlington, MA, USA) with a series of membranes (Merck-Millipore, Burlington, MA, USA). Wastewater samples were graded into six MW fractions, which were MW > 100 kDa, 100 kDa > MW > 30 kDa, 30 kDa > MW > 10 kDa, 10 kDa > MW > 5 kDa, 5 kDa > MW > 1 kDa, and MW < 1 kDa, under a constant high-purity nitrogen gas (99.999%) pressure

of 0.1 MPa. During the process, a blank sample for each membrane module consisting of deionized water was also collected before sample application [24].

2.3.4. Polarity Fraction

DOM was divided into HPI, HPO, and TPI based on the hydrophilic–hydrophobic properties of resin columns XAD-4 and XAD-8 (Supelco, Bellefonte, PA, USA) [24]. Firstly, the water sample was acidified to pH 2.0 with 1.0 mol L^{-1} HCl, then passed through XAD-8 and XAD-4 resin columns in turn at the flow rate of 2.00 mL min^{-1}. The effluent collected was designated the HPI. Secondly, HPO and TPI were eluted from XAD-8 and XAD-4 resin columns with 0.1 mol L^{-1} NaOH at the flow rate of 1.00 mL min^{-1}, respectively. Finally, the three abovementioned fractions were adjusted to pH 7.0 by 1.0 mol L^{-1} HCl or 1.0 mol L^{-1} NaOH. The abovementioned fractions were stored at 4 °C in amber glass bottles.

2.4. DBPs Formation of DOM

Wastewater samples were diluted to 1.0 mg L^{-1} DOC by phosphate buffer solution (10 mmol L^{-1}, pH is 7.0 ± 0.2). The chlorine solution at the concentration of 8 mg Cl_2 (mg DOC)$^{-1}$ was added to the samples to ensure at least 2.0–3.0 mg L^{-1} residual free chlorine after 72 h. Finally, the samples were kept at 25 °C in the dark. After a contact time of 72 h, the residual chlorine was measured using the N, N-dethyl-p-phenylenedi-amine (DPD) colorimetric method, and then the samples were quenched with 200 µL of 0.2 mol L^{-1} ascorbic acid [32].

Four THM_s ($CHCl_3$, $CHBrCl_2$, $CHBr_2Cl$, and $CHBr_3$) species, two HK_s (1,1-DCP and 1,1,1-TCP) species, four HAN_s (TCAN, DCAN, BCAN, and DBAN) species, one HNM (TCNM) specie and CH (chloral hydrate) were extracted by liquid-liquid extraction (LLE) with methyl tert-butyl ether (MTBE) and analyzed according to US EPA method 551.1, respectively [33]. Nine HAA_s (MCAA, MBAA, DCAA, TCAA, BACC, DBAA, BDCAA, DBCAA, and TBAA) species were extracted by LLE with MTBE followed by being derived with acidic methanol according to USEPA method 552.3 [32]. DBPs were measured by a gas chromatograph (GC) (GC-2014, Shimadzu, Japan) with an HP electron capture detector (ECD). The column was an Agilent HP-5 capillary column (30 m × 0.25 mm I.D., 0.25 µm film thickness).

3. Results and Discussion

3.1. Changes in the Characteristics of DOM

3.1.1. Water Quality

As shown in Table 1, the concentration of DOC of the influent and effluent were 112.9 mg L^{-1} and 11.21 mg L^{-1} in the WWTP. The total removal rate was 89%, indicating that this process has a good removal efficiency of organic matter. Moreover, it is mainly the joint action of microbial degradation and membrane interception. The concentration of NH_4^+-N in the AGC was reduced from 21.32 mg L^{-1} to 17.9 mg L^{-1}, whereas the concentration of DON was reduced from 8.74 mg L^{-1} to 6.02 mg L^{-1}, owing to NH_4^+-N forming to NO_3-N and NO_2-N by ammoniation in aeration conditions. After the AAO treatment, the concentration of DON was reduced to the lowest, which was only 0.09 mg L^{-1}, and NH_4^+-N decreased to 1.92 mg L^{-1}. In the MBR effluent, NH_4^+-N reached the minimum of 0.3 mg L^{-1}, and the concentration of DON increased to 3.83 mg L^{-1}. SUVA value showed an increasing trend, from 0.25 to 1.24 L (m·mg)$^{-1}$, indicating that the unsaturated double bond and the aromatic substance were produced.

Table 1. Water quality indexes of influent and effluent of main sewage treatment unit in WWTP.

Parameter	Influent	Primary Sedimentation Tank Effluent	Biological Treatment Process Effluent	MBR Effluent
DOC (mg L^{-1})	112.90	64.13	47.78	12.21
DTN (mg L^{-1})	31.54	25.00	7.95	13.95
NH_4^+-N (mg L^{-1})	21.32	17.90	1.92	0.30
NO_3-N (mg L^{-1})	1.46	1.08	5.88	9.82
NO_2-N (mg L^{-1})	0.01	0.01	0.06	0.01
DON (mg L^{-1})	8.74	6.02	0.09	3.83
UV_{254} (cm^{-1})	0.28	0.17	0.25	0.15
SUVA (L $(m \cdot mg)^{-1}$)	0.25	0.26	0.52	1.24
DON/DOC	0.08	0.09	0.01	0.29

Due to the presence of macromolecular aromatic organics with certain biological toxicity in the raw water, the removal effect of microorganisms is not ideal. It might also be that organic substances with an aromatic structure are generated during microbial metabolism. Although aromatic substances might be produced during microbial metabolism, the removal rate of UV_{254} in MBR was still 40%, mainly due to the efficient interception of membrane modules. The results show that AAO and MBR could remove DOC, DON, and other organics well, but the removal effect of aromatic DOM was poor, and the overall effluent quality was good. The reason might be because, during AAO and MBR process, bacteria achieve pollutant biosorption and continuous biodegradation [34,35], the low MW DOM was easy to be degraded, but the refractory humic-like, tryptophan-like, and protein-like materials were accumulated [23].

3.1.2. Three-Dimensional EEM Analysis of DOM

The proportion of regional I was dominant both in the influent and effluent of each processing unit (Table 2 and Figure 2). After the primary sedimentation tank and biological treatment process, the proportion of regional I basically remained unchanged. While the proportion of region I decreased from 65.46% to 47.97% after membrane separation, indicating that the membrane separation can effectively remove protein compared with the biological treatment process, mainly lysine and tryptophan substances. It means that MBR can remove protein-like substances effectively; this was consistent with Meng et al. [22]. The proportion of region II was small, accounting for 5.65%~6.34%. After treatment in the AGC, the proportion of region III increased from 24% to 25.2%, indicating that SMPs were produced, mainly due to the presence of aerobic microbial. On the other hand, after treatment in the AAO process, the region III increased from 25.2% to 26.3%, indicating that more SMPs were produced. After membrane filtration, the regional III accounted for 33%, probably because of the high concentration of microorganisms and a large amount of aeration. Moreover, the membrane hole is 0.1 μm, and SMPs can pass through it. In the process of sewage treatment, the area IV increased from 1.68% to 3.05%, mainly due to the relatively stable structure of humic acid, which cannot be used by microorganisms, resulting in the accumulation of humic acid substances. Thus, the MBR membrane cannot intercept humus substances well compared with protein, consistent with Wang and Chen [23].

Table 2. FRI parameters for operationally defined 3D-EEM regions and volumetric (φ) and percentage (*p*) values for 3D-EEM analysis of the wastewater samples.

FRI Parameters			EEM Analysis							
EEM Region	Projected Excitation-Emission Area (nm^2)	Mfi	Influent		Primary Sedimentation Tank Effluent		Biological Treatment Process Effluent		MBR Effluent	
			$\varphi_{i,n}$ ($\times 10^5$)	$P_{i,n}$ (%)	$\varphi_{i,n}$ ($\times 10^5$)	$P_{i,n}$ (%)	$\varphi_{i,n}$ ($\times 10^5$)	$P_{i,n}$ (%)	$\varphi_{i,n}$ ($\times 10^5$)	$P_{i,n}$ (%)
I	5000	0.16	28.93	67.67	36.58	67.32	31.22	65.46	87.26	47.97
II	6250	0.21	2.71	6.34	3.07	5.65	2.84	5.96	8.96	5.95
III	2500	0.08	10.39	24.30	13.68	25.17	12.53	26.29	49.72	33.03
IV	16,675	0.55	0.72	1.68	1.02	1.87	1.09	2.30	4.60	3.05
Sum	30,175	1.00	42.75	100.00	54.34	100.00	47.68	100.00	150.53	100.00

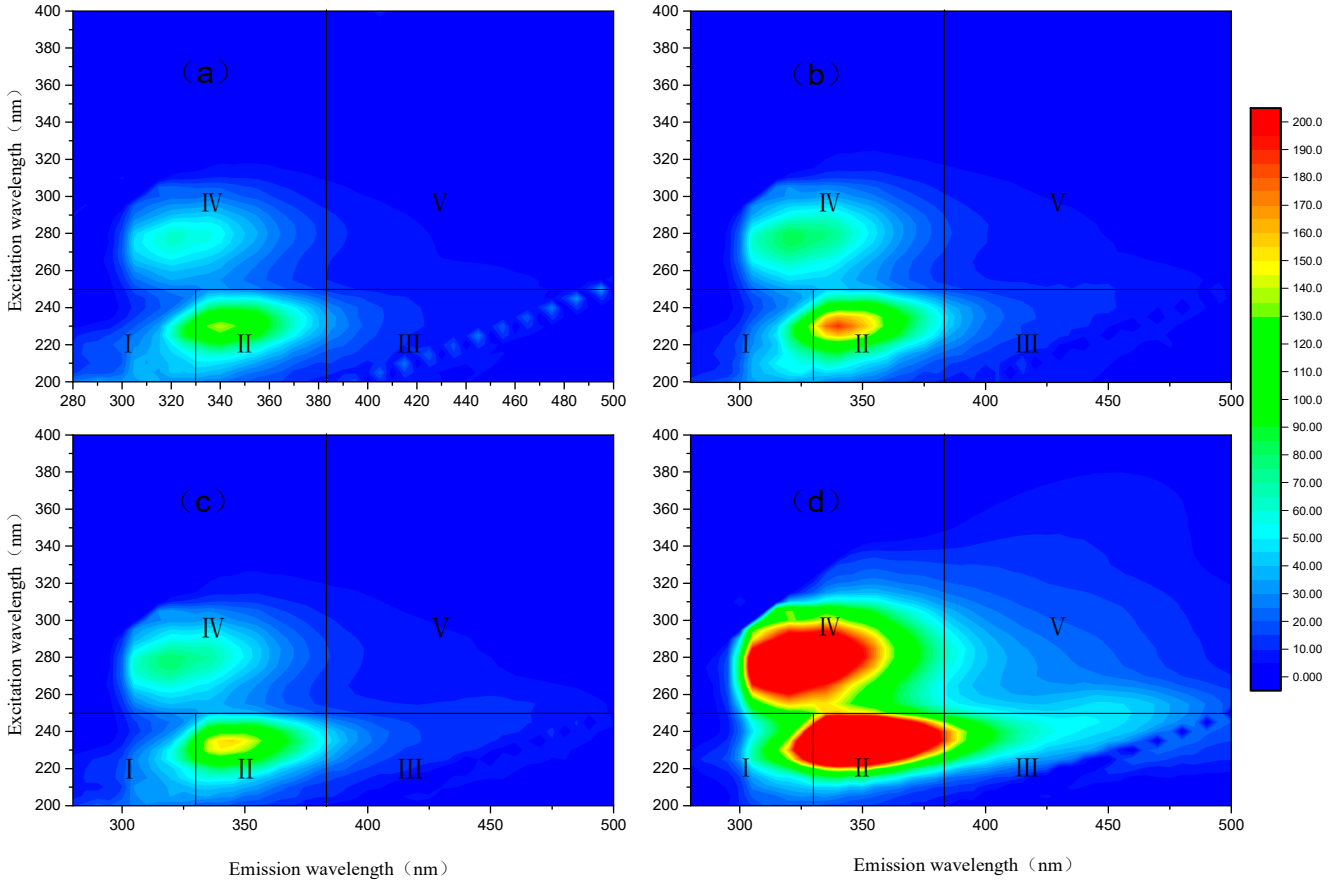

Figure 2. Three-dimensional EEM of DOM in AAO-MBR treatment process: (**a**) Influent, (**b**) AGC effluent, (**c**) AAO effluent, and (**d**) MBR effluent.

Therefore, the proportion of regional I decreased from 67.67% to 47.97% during the whole sewage treatment process and MBR with the highest removal rate. In comparison, the proportion of regional III increased from 24.30% to 33.03% during the whole sewage treatment process, mainly due to the accumulation of MBR treatment. Similarly, the proportion of regional IV increased from 1.68% to 3.05%, mainly due to the accumulation of the biological treatment. SMP is a main fraction of DOM and can be released by microbial metabolism during biological wastewater treatment.

3.1.3. FT-IR Analysis of DOM

After the treatment of AGC, the wave numbers 1110 cm^{-1} (including phenolic, lipid, ether, phenol, linear alcohol, and other substances related) and 1644 cm^{-1} (related to

the C=O aromatic species) decreased. It was indicated that the aromatic and long-chain aliphatic organic compounds might be removed (Figure 3). At the same time, the wave number of 980 cm^{-1} (mainly polysaccharide C-O vibration) also decreased, probably due to the removal of hydrophilic carbohydrate substances. After the biological treatment, the wave number increased from 1644 cm^{-1}, 1100 cm^{-1}, and 980 cm^{-1}, indicating that the aroma and polysaccharides of the water increased. After the treatment of the MBR process, the absorbance at 1100 cm^{-1} and 980 cm^{-1} decreased, indicating that the long-chain aliphatic substances and polysaccharides had been effectively removed. The results were consistent with the 3D-EEM data showing that the MBR effluent contained more fulvic acid-like substances (region II). Meng et al. [22] reported that the proportion of high MW polysaccharide, humus, and primary amine in the MBR effluent was higher than that in the AAO effluent. They also found that the peak value at 1620 cm^{-1} (C=O stretching) in the MBR effluent was stronger than in the AAO effluent, which was contrary to our results. The reason might be that the changes in DOM were related to operating conditions, including SRT, HRT, carbon source, etc. [23].

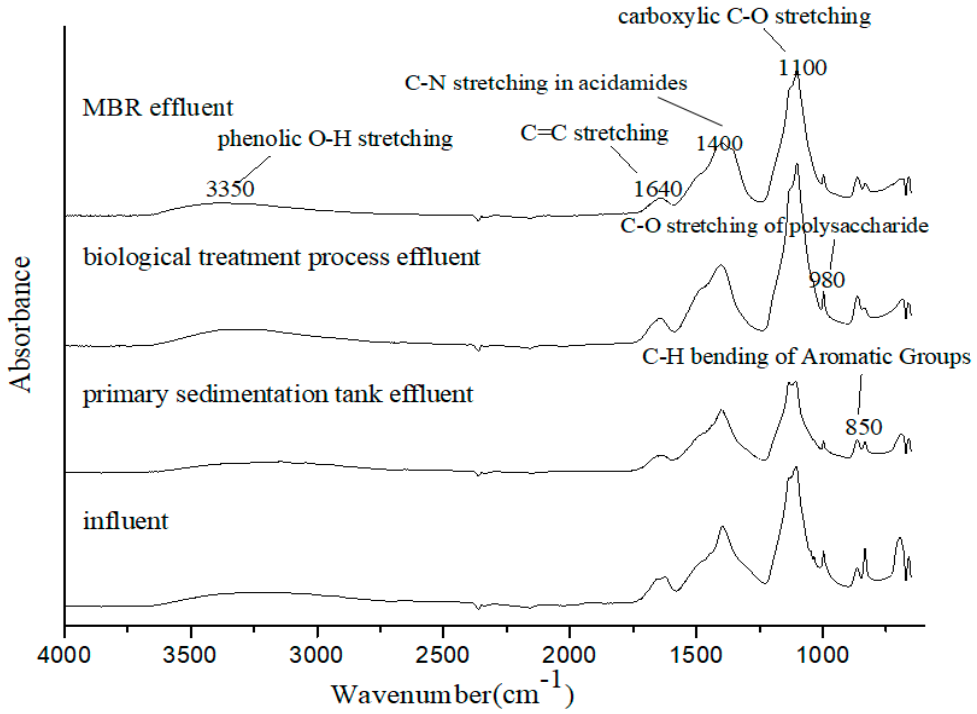

Figure 3. FT–IR spectra of the WWTP.

3.1.4. ^{1}H-NMR Analysis of DOM

As Figure 4 shows, δ_H = 0.6–1.8 (H–C) on behalf of the proportion of aliphatic compounds has been reduced after sewage treatment, indicating that the AAO-MBR process can be removed by aliphatic compounds as well, which was consistent with the results of FT-IR spectrum. In addition, the peak area of δ_H = 3.2–4.1 (H–C–O) decreased after the AGC. Furthermore, after the AAO process and MBR process, the peak area of δ_H = 3.2–4.1 increased, indicating that the water content of oxygen was removed by the AGC, other than producing hydroxyl, esters, and ethers, greatly produced after the biological treatment process and MBR treatment. The reason might be that the aroma and polysaccharides of the water increased after the AAO treatment, whereas the long-chain aliphatic substances and polysaccharides have been effectively removed through MBR treatment.

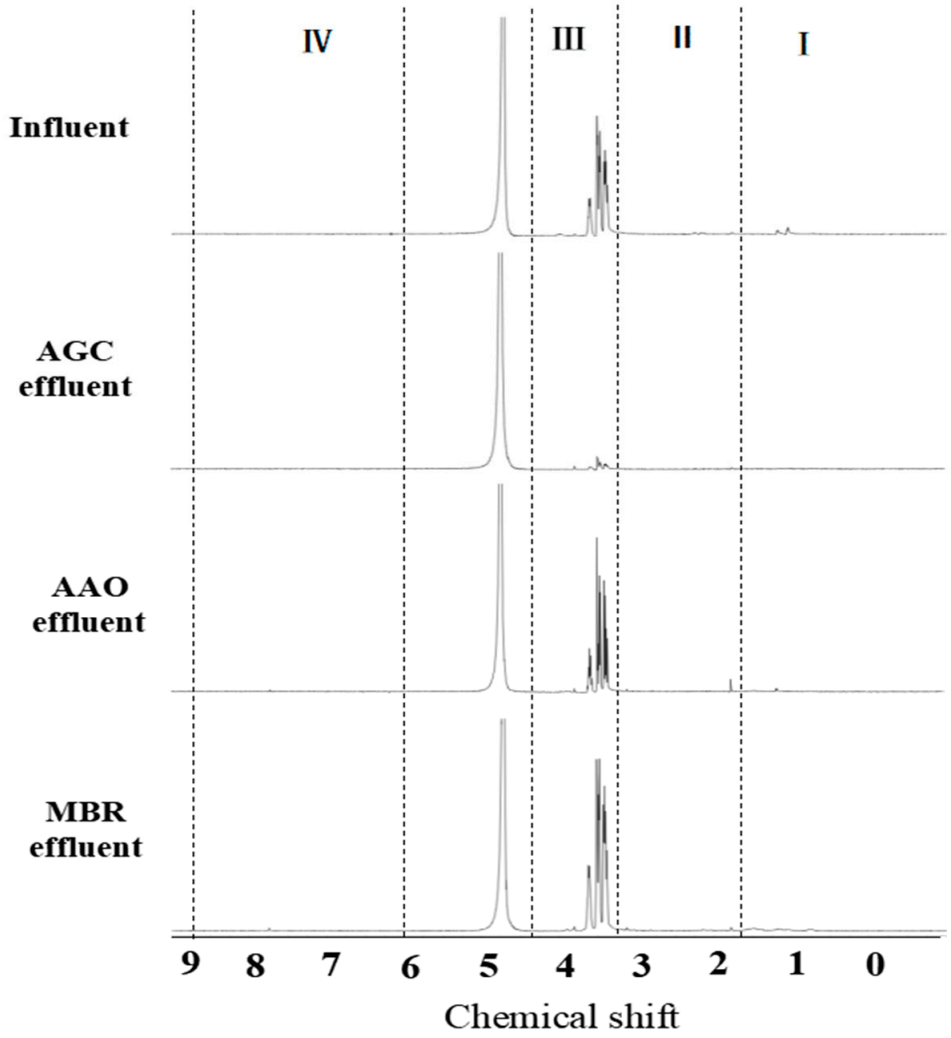

Figure 4. ^{1}H-NMR spectra of the WWTP.

3.1.5. Molecular Weight Fractions

The MW fraction >5 kDa fraction was dominant, contributing about 74.19% of the total DOC in the AGC effluent, while the MW fraction of 1–5 kDa was small, accounting for 9.89% (Figure 5a). As the physical removal process, AGC has less influence on the MW distribution and hydrophilic–hydrophobic properties of sewage. After the AAO process, the high MW fractions (MW > 10 kDa) decreased from 61.13% DOC to 22.17% DOC, and the low MW fractions (MW < 5 kDa) significantly increased from 38.87% DOC to 77.83% DOC, mainly due to microorganisms produced SMPs during substrate metabolism and bacterial growth [21]. After the MBR process, the MW distribution shows a bimodal trend as a whole. The macromolecule material increased significantly, >100 kDa fraction increased from 8.56% to 20.97%, 10~30 kDa fraction increased from 4.73% to 12.75%, meanwhile, and the small molecular material has been reduced, especially the <1 kDa component was reduced from 40.48% to 24.53%. The effluent of the AAO treatment contains more MW < 1 kDa fractions than the MBR effluent, which was different from the results of Meng et al. [22]. The different MW distribution during MBR treatment may be caused by different operational conditions. It was reported that the high MW fraction in SMPs increased with the increase in SRT [23]. Lower MW (<5 kDa) accounted for 92.43% of DOM with an SRT of 10 d, and higher MW fractions dominated DOM with higher SRT [36].

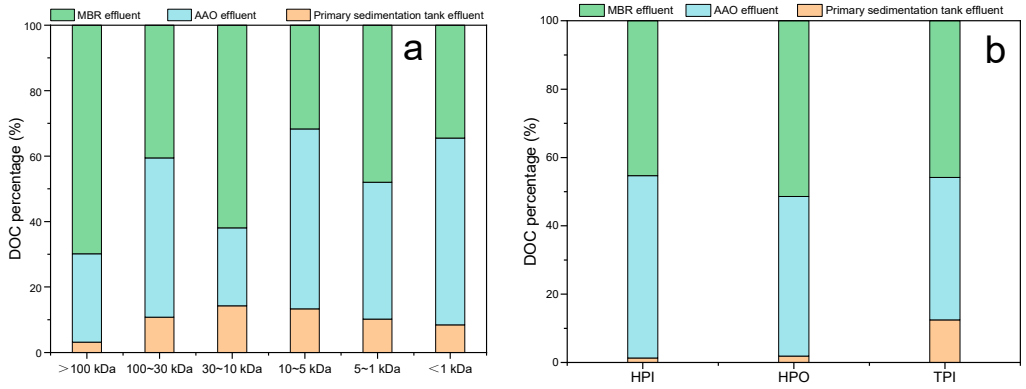

Figure 5. DOC percentage of various MW fractions (**a**) and hydrophobicity fractions (**b**) (HPI: hydrophilic fraction; HPO: hydrophobic fraction; TPI: transphilic fraction).

Due to different SRT, the conclusion about the MW distribution of DOM in MBR treatment may be contradictory. Since MBR is generally operated at high SRT and biomass concentrations, the generation of SMPs was mainly attributed to microbial decay through endogenous respiration [21]. SMPs are generally classified into two categories: utilization-associated products (UAPs) derived from the biodegradation of the original substrate in the microbial growth phase and biomass-associated products (BAPs) released during biomass decay in the endogenous phase. UAPs are mostly composed of low MW materials, while BAPs contain more of the high MW components [21]. Thus, the AAO process contains more UAP, and the MBR contains more BAP [31]. Microorganisms in MBR treatment at high SRT tend to produce more high MW SMPs and remove more initial organic matter through cell lysis in endogenous respiration [37]. The MBR process shows much longer SRT than the AAO process, leading to degrading more initial organic matter and forming more of the high MW SMPs. Therefore, the MBR effluent contains more MW > 1 kDa fractions than the AAO effluent.

3.1.6. Polarity Fractions

As shown in Figure 5b, the main components of the AGC effluent were HPI and HPO, of which HPI accounted for 72.51%, followed by HPO accounting for 22.41%. After the AAO process, the HPI decreased significantly to 42.74%, and the proportion of HPO fraction increased to 48.55%, TPI increased to 8.71% slightly, mainly due to the role of microorganisms in the use of HPI substances to produce HPO SMPs. After the MBR process, HPI was reduced to the lowest, with a value of 33.41%, and the HPO increased to 55.11%. The reason might be that many HPO SMPs were generated and released through microbial metabolic activities in the bioreactor under high SRT and biomass concentrations.

Some studies thought that pH affects the hydrophobicity of DOM more sensitively than MW distribution [22]. Low pH results in the generation of HPO [38]. The MBR process produced more SMPs and HPO fractions, which can be derived from cell lysis and extracellular polymeric substance [23]. It was reported that AAO treatment produced more content of hydrophobic protein [22]. In comparison, MBR with longer SRT captured HPO and produced more hydrophilic polysaccharides than AAO treatment.

3.2. Formation of DBPs during Chlorination

3.2.1. Changes in C-DBPFP

The species of C-DBPFPs was dominated by THMs and HAAs (Figure 6a). The HAAs value of influent water was 5.3 μg (L·mg C)$^{-1}$ and reduced by 27% after the AGC process. Compared with the influent of the AAO unit, the HAAs of the AAO effluent increased by 4.8 times, which increased to 17.1 μg (L·mg C)$^{-1}$. After the MBR process, the HAAs were further increased substantially with the value of 22.3 μg (L·mg C)$^{-1}$ for an increase of 30%. The results show that the AAO process may promote the formation of the HAA precursor.

There has been an upward trend of THMs during the AAO-MBR process. The THMs value of influent water was 12.9 μg (L·mg C)$^{-1}$ and increased to 30.6 μg (L·mg C)$^{-1}$ after the AGC; the THM precursor increased by 1.37 times. After the AAO treatment, the THMs increased to 77.5 μg (L·mg C)$^{-1}$, and the THM precursor increased by 1.53 times. The maximum amount of THMs was 128.3 μg (L·mg C)$^{-1}$ in the MBR effluent. The formation potentials of HKs showed a similar trend with THMs, and the maximum amount was 12.4 μg (L·mg C)$^{-1}$. CH had a low level, with a value of 9.7 μg (L·mg C)$^{-1}$, which accounted for 5% percent of C-DBPFP. In addition, C-DBPFP showed a rising trend, possibly due to the increase in SUVA.

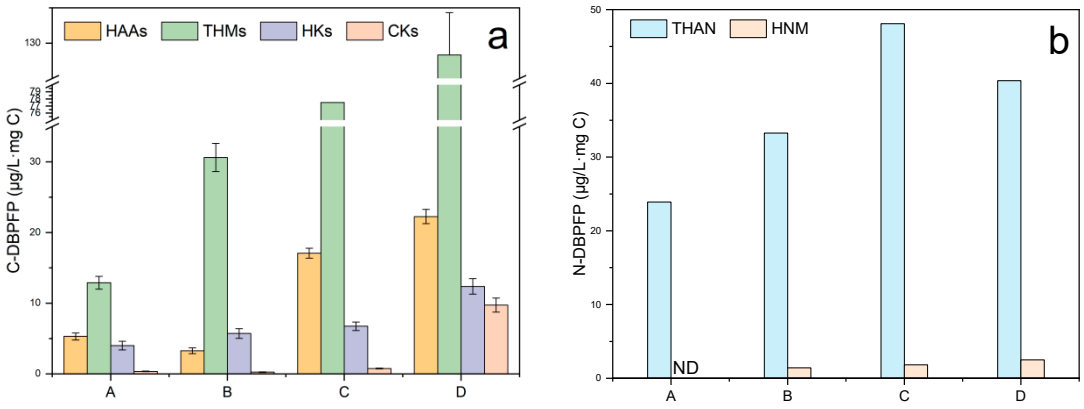

Figure 6. DBPFP of the WWTP ((**a**) the formation of C-DBPFP; (**b**) the formation of N-DBPFP;) (A: influent of wastewater, B: AGC effluent, C: AAO effluent, and D: MBR effluent).

During wastewater treatment, the amount of C-DBPs in the effluent was increased, which means that the C-DBPs precursors were increased (Figure 6a). The change in DBPFP depended on the change in DBPs precursors [39], which was consistent with our study. The yields of C-DBPs in the MBR effluent were higher than in the AAO effluent. Meng et al. [22] found that the halogenated DBP of the MBR effluent was higher than that of the AAO effluent, especially TCM. When SMPs are chlorinated, C-DBPs and N-DBPs can be formed simultaneously [21]. It is reported that C-DBPFP has a positive linear correlation with the combination ratio of aromatic C and C-O, which are the main precursors for the formation of C-DBP [40].

3.2.2. Changes in N-DBPFP

HNM was not detected in the influent water. The changing trend of N-DBPFP was increased first and then decreased in the AAO-MBR process (Figure 6b). It was indicated that the N-DBP precursor increased first after the AGC and AAO treatment and then decreased after the MBR process per DOC. The HANs were 23.09 μg (L·mg C)$^{-1}$ in influent; after the AGC increased to 33.26 μg (L·mg C)$^{-1}$, the HAN precursors increased by 1.44 times, which might be due to the increase in humus acids and SMPs. After the AAO treatment, the HANs further increased to 48.09 μg (L·mg C)$^{-1}$, an increase of 1.45 times; this might be due to a large number of humus acids, SMPs, and polysaccharides that existed in the AAO effluent. However, after the MBR process, the HAN has been reduced to 40.36 μg (L·mg C)$^{-1}$. With the progress of the process, HNM showed an increasing trend, the maximum value of 2.49 μg (L·mg C)$^{-1}$, but accounted for less. DON, including aromatic N, amide/peptide N, and primary amine N, is the precursor of N-DBPs. Moreover, N-DBPFP has a positive linear correlation with the concentration of DON [40]. Amino acids play a key role as precursors of HANs and cyanogen halides. It has been proved that aspartic acid, tryptophan, and canine could produce DCAN [41].

3.3. Contributions of DBP Formation Potential from MW Fractions and Polarity Fractions

3.3.1. C-DBPFP of MW Fractions and Polarity Fractions

In the AGC effluent, the >100 kDa fraction had the largest C-DBPFP with the value of 51.41 μg (L·mg C)$^{-1}$, the HPI fraction had the largest C-DBPFP with the value of 51.69 μg (L·mg C)$^{-1}$, and macromolecular hydrophilic substances accounted for the most (Figure 7a). Macromolecular hydrophilic substances were the main precursors for the AGC effluent. After the AAO process, the percentage of low MW fractions (MW > 5 kDa) increased from 38.87% to 77.83%. The >5 kDa fraction contributed from 22.28% up to 71.22% of the total C-DBPFP (Figure 7c). Moreover, the percentage of HPO fractions increased from 22.41% to 48.55%, while the HPO fraction contributed from 34.02% to 58.72% of the total C-DBPFP (Figure 7d). After the MBR process, >30kDa fractions were increased from 17.44% to 29.56% of the total DOC with a high value of C-DBPFP (Figure 7a). The >30 kDa fraction also contributed from 22.27% to 39.90% of the total C-DBPFP (Figure 7d). On the contrary, the <5kDa fraction decreased from 60.93% to 47.92% of the total DOC with a low value of C-DBPFP (Figure 7a). Furthermore, the <5 kDa fraction contributed from 47.99% to 38.93% of the total C-DBPFP (Figure 7d). In addition, in the MBR effluent, the HPO fraction contributed from 58.72% to 67.65% of the total C-DBPFP.

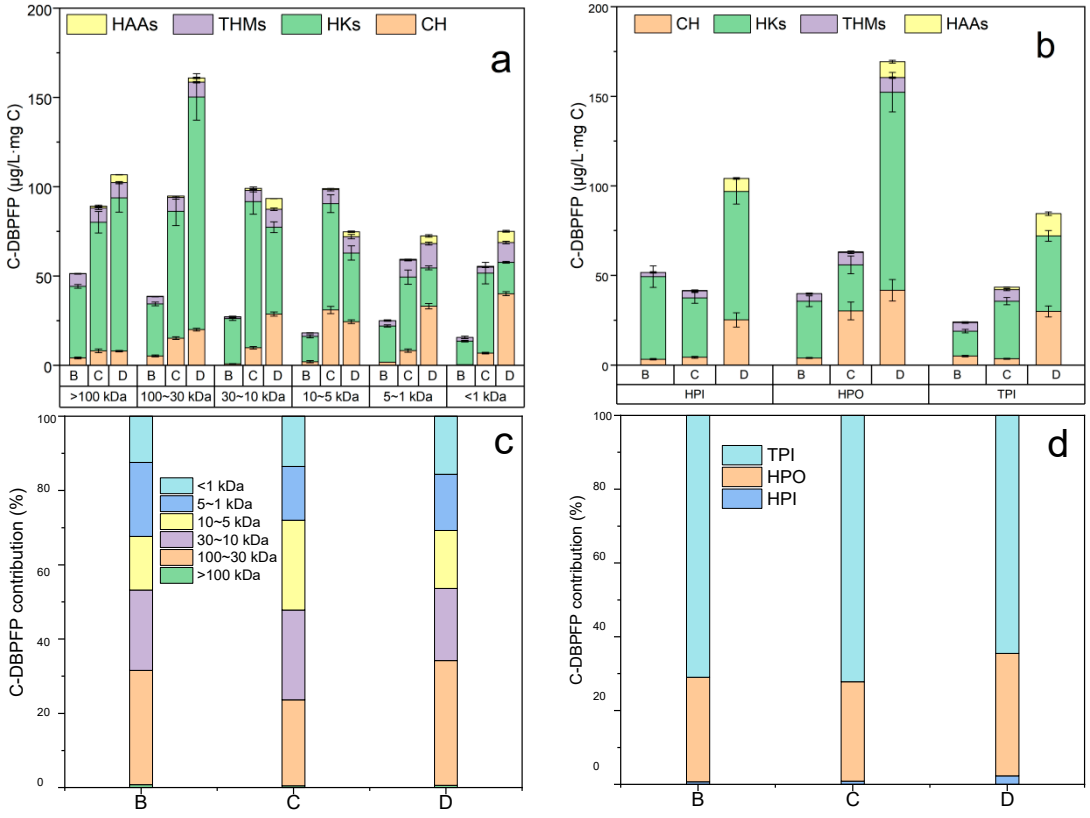

Figure 7. C-DBPFP of MW fractions and polarity fractions and their contributions for diffident fractions after chlorination (**a**) C-DBPFP of MW fractions; (**b**) C-DBPFP of polarity fractions; (**c**) C-DBPFP contribution of MW fractions; (**d**) C-DBPFP contribution of polarity fractions) (B: AGC effluent, C: AAO effluent, and D: MBR effluent).

As mentioned above, low MW and hydrophobic DOM was the primary source of C-DBPs precursors in the AAO effluent. In comparison, high MW DOM and hydrophobic was the primary source of C-DBPs precursors in the MBR effluent. The low MW and HPO DOM were mainly SMPs, which were derived from the biodegradation of the original substrate in the microbial growth phase. In addition, due to polysaccharides, humus substances increased, and the C-DBPFP also increased. During wastewater treatment, humic fractions with relatively higher MW were considered refractory organic matter.

SMP is a main fraction of DOM, which can be released by microbial metabolism during biological wastewater treatment [23]. DOM in the MBR effluent was mainly fulvic acids, polysaccharides, and primary amines, while DOM in the AAO effluent was mainly SMPs, proteins, and amino acids, especially secondary amines [22].

3.3.2. N-DBPFP of MW Fractions and Polarity Fractions

The N-DBPFP of the macromolecule organic was higher in the AGC effluent, where the >10 kDa fraction accounted for 61.13% of the total DOC, the contribution rate in the >10 kDa fraction was 66.31% of the total N-DBPFP (Figure 8a). The N-DBPFP of the HPI fraction was higher in the AGC effluent and accounted for 72.5% of the total DOC; the contribution rate in the HPI fraction was 74.93% of the total N-DBPFP (Figure 8b). Thus, macromolecules of HPI DOM were the primary source of N-DBPs precursors in the AGC effluent, and it might be a readily degradable organic substance left in the water. After the AAO process, low MW fractions (<5 kDa) contributing from 23.06% to 69.11% of the total N-DBPFP was attributed to 60.94% of the total DOC, and high N-DBPFP in low MW fraction. The N-DBPFP was higher in HPO fractions, and the HPO fraction was 48.55% of the total DOC (Figure 8b). It is suggested that the low MW hydrophobic substance was the main precursor of N-DBPs in the AAO effluent.

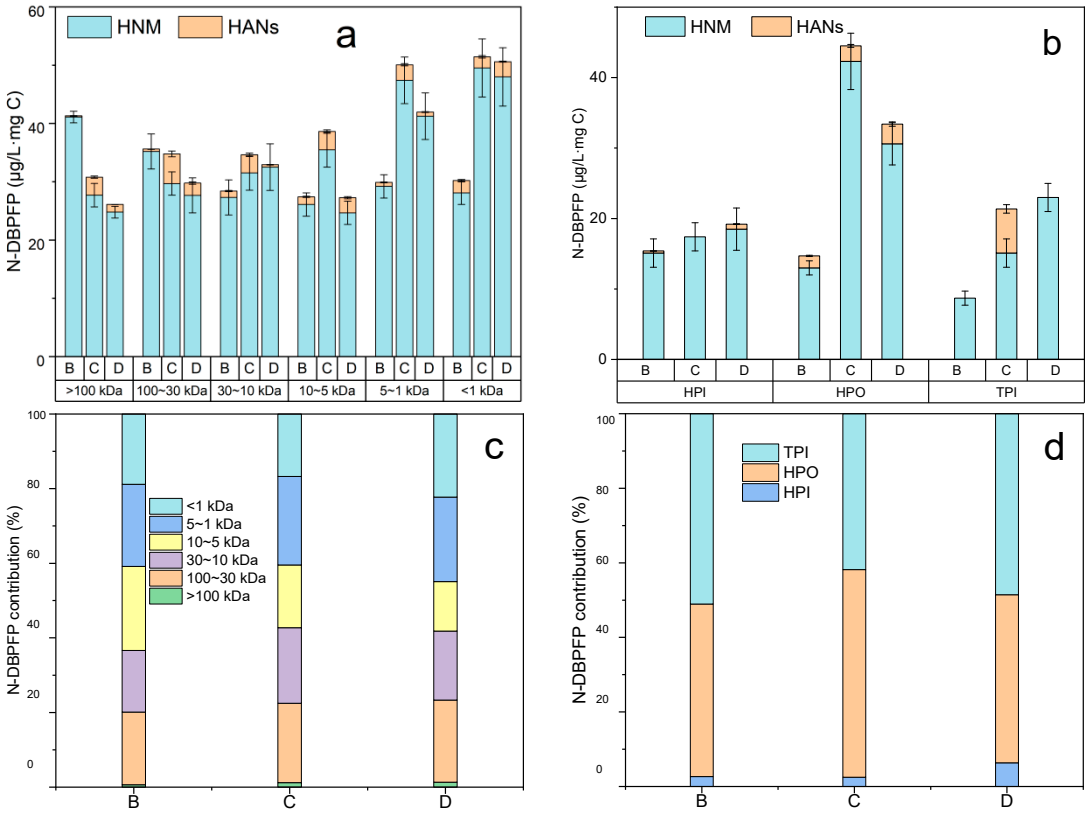

Figure 8. N-DBPFP of MW fractions and polarity fractions and their contributions for diffident fractions after chlorination (**a**) N-DBPFP of MW fractions; (**b**) N-DBPFP of polarity fractions; (**c**) N-DBPFP contribution of MW fractions; (**d**) N-DBPFP contribution of polarity fractions) (B: AGC effluent, C: AAO effluent, and D: MBR effluent).

According to the previous 3D-EEM analysis, low MW hydrophobic substances were mainly hydrophobic SMPs. After the MBR process, the N-DBPFP in the low MW fraction was more than in the high MW fraction. Since the generation time of the N-DBPFP was slower than the C-DBPFP, the reaction time with macromolecule was longer compared with low MW. Due to high SRT and microbial concentration, the MBR process produces more macromolecular refractory SMPs. Small molecules accounted for less proportion, and

N-DBPFPs were reduced. The <5 kDa fraction contributed to 55.24% of the total N-DBPFP, HPO fraction contributed to 67.09% of the total N-DBPFP. It can be concluded that small MW hydrophobic DOM were the primary source of N-DBP precursors in the MBR effluent.

3.4. Changes in C-DBP and N-DBP Yields

As shown in Figure 9, C-DBP yield was increased from 2474.33 μg L^{-1} to 2554.81 μg L^{-1} after the AGC due to the high-value C-DBPFP, mainly due to the increase in SMPs and humus acids. The N-DBP yield was reduced to 2223.11 μg L^{-1}, mainly with the result of DOC being removed. The results indicate that in the AGC, 3% C-DBP precursor was produced, and 17% N-DBP precursor was removed. The AAO process could remove the DOM in the water by microbial action, with the DOC removal rate obtaining 25.5%. However, increased polysaccharides and small molecule SMP substances are predominantly DBP precursors. C-DBP yields up to 4877.31 μg L^{-1}, and N-DBP yields up to 2384.81 μg L^{-1}, indicating that in the AAO process, C-DBP and N-DBP precursor was produced, 90% and 7%, respectively. The MBR process removed 74.4% DOC, so the C-DBP yield was reduced to 2108.66 μg L^{-1}, and the N-DBP yield was reduced to 523.40 μg L^{-1}. In the MBR process, 56.8% C-DBP precursor was removed, and 78.1% N-DBP precursor was removed. The yields of HANs and TCNM in the MBR effluent were higher compared with the AAO effluent, which was consistent with the results of Meng et al. [22]. Fan et al. [42] reported that sand filtration resulted in an average increase of 14.8% in organic compounds, especially 28.59% in aromatic protein II and 18.7% in SMPs, due to the metabolism by microorganisms present in the filter. Shen et al. [43] reported that the DBPFP yield increased the generation of SMPs by BAC.

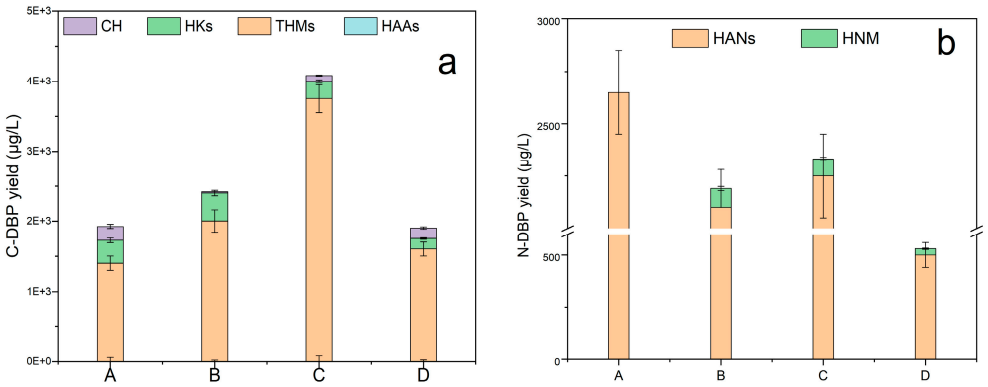

Figure 9. C-DBP and N-DBP yield of water samples (**a**) C-DBP yield; (**b**) N-DBP yield) (A: influent of wastewater, B: AGC effluent, C: AAO effluent, and D: MBR effluent).

AGC and AAO units promoted the formation of DBPs precursors. At the same time, 56.8% of the C-DBP precursor and 78.1% of N-DBP precursor were removed in the MBR process, which was due to the high removal efficiency of DOC (removal rate of 74.4%) at the MBR unit due to the efficient interception of DOC by the MBR membrane. The process dominated by microbial degradation has no significant effect on the removal of precursors of DBPs. The increased precursors at the biodegradation unit could be explained by macromolecular degradable substances that were degraded to small molecular SMPs, which were the main precursor of C- and N-DBP. However, the MBR membrane has a better interception effect on macromolecular organic matter and a poor removal effect on small molecular organic matter. Some studies have shown that reverse osmosis membrane has an obvious effect on the removal of small molecular organics.

4. Conclusions

Quite effective in removing DOC and NH_4^+-N in wastewater was efficiently removed via the AAO-MBR treatment process with removal efficiencies of 89% and 98%. MW distribution and hydrophilic-hydrophobic properties of DOM were changed in the AAO-MBR

treatment process. Small molecule hydrophobic SMPs, humus, and polysaccharides were increased in the AAO process, while large molecule hydrophobic SMPs and humus were increased in the MBR process. DOM in the AAO effluent contained high concentrations of C- and N-DBPFP in low MW and HPO fractions. Regarding DOM in the MBR effluent, C-DBPFP was mainly high MW and HPO fractions, but low MW and HPO fractions of N-DBPFP were observed. The precursors of C-DBP and N-DBP increased by 90.9% and 7.3%, respectively, after the AAO treatment. In total, 56.8% of the C-DBP precursors and 78.1% of N-DBP precursors were removed in the MBR process due to the high removal efficiency of DOC (removal rate of 74.4%) at the MBR unit. The increased precursors at the AAO unit could be explained by macromolecular degradable substances that were degraded to small molecular SMPs, which were the main precursor of C- and N-DBP. Regarding the MBR unit, the total amount of DBPs decreased due to the high DOC removal rate. However, there were still C- and N-DBPs precursors (e.g., hydrophobic SMPs and small molecular substances) that reacted with chlorine in the MBR. The obtained results can provide a reference for the regulation of DBPs in wastewater reuse.

Author Contributions: All authors contributed to the study's conception and design. Material preparation, data collection, and analysis were performed by X.R., F.W., Y.Z., J.W. and H.M. The first draft of the manuscript was written by X.R. and F.W. and all authors commented on previous versions of the manuscript. X.R. and F.W. contributed to the work equally. All authors have read and agreed to the published version of the manuscript.

Funding: The study was supported by the National Natural Science Foundation of China (NSFC) (No. 42207466), the Natural Science Foundation of Jiangsu Province (BK20221103), the National Natural Science Foundation of China (NSFC) (general program) (No. 42177376), and the national major science and technology projects for water pollution control and treatment (2017ZX07204001-02).

Institutional Review Board Statement: This manuscript was original research that has not been published previously and is not in consideration for publication elsewhere, in whole or in part. This experiment does not involve human or animal tests.

Informed Consent Statement: Not applicable.

Data Availability Statement: All data included in this study are available upon request by contact with the corresponding author.

Conflicts of Interest: The authors have no relevant financial or nonfinancial interests to disclose.

References

1. Wang, Z.; Yang, Y.; Xiang, W.; Wu, B.; Cui, X.; Zhou, Y. Performance and mechanisms of greywater treatment in a bio-enhanced granular-activated carbon dynamic biofilm reactor. *Npj Clean Water* **2022**, *5*, 56. [CrossRef]
2. Zhou, Y.; Li, R.; Guo, B.; Zhang, L.; Zou, X.; Xia, S.; Liu, Y. Greywater treatment using an oxygen-based membrane biofilm reactor: Formation of dynamic multifunctional biofilm for organics and nitrogen removal. *Chem. Eng. J.* **2020**, *386*, 123989. [CrossRef]
3. Zhou, Y.; Anwar, M.N.; Guo, B.; Huang, W.; Liu, Y. Response of antibiotic resistance genes and microbial niches to dissolved oxygen in an oxygen-based membrane biofilm reactor during greywater treatment. *Sci. Total Environ.* **2022**, *833*, 155062. [CrossRef]
4. Richardson, S.D.; Kimura, S.Y. Water analysis: Emerging contaminants and current issues. *Anal. Chem.* **2020**, *92*, 473–505. [CrossRef] [PubMed]
5. Yang, M.; Zhang, X.; Liang, Q.; Yang, B. Application of (LC/) MS/MS precursor ion scan for evaluating the occurrence, formation and control of polar halogenated DBPs in disinfected waters: A review. *Water Res.* **2019**, *158*, 322–337. [CrossRef] [PubMed]
6. Zhou, H.; Tian, L.; Ni, M.; Zhu, S.; Zhang, R.; Wang, L.; Wang, M.; Wang, Z. Effect of dissolved organic matter and its fractions on disinfection by-products formation upon karst surface water. *Chemosphere* **2022**, *308*, 136324. [CrossRef] [PubMed]
7. Wu, M.; Liang, Y.; Peng, H.; Ye, J.; Wu, J.; Shi, W.; Liu, W. Bioavailability of soluble microbial products as the autochthonous precursors of disinfection by-products in aerobic and anoxic surface water. *Sci. Total Environ.* **2019**, *649*, 960–968. [CrossRef] [PubMed]
8. Xu, X.; Kang, J.; Shen, J.; Zhao, S.; Wang, B.; Zhang, X.; Chen, Z. EEM–PARAFAC characterization of dissolved organic matter and its relationship with disinfection by-products formation potential in drinking water sources of northeastern China. *Sci. Total Environ.* **2021**, *774*, 1–9. [CrossRef]
9. Chang, H.; Chen, C.Y.; Wang, G. Characteristics of C-, N-DBPs formation from nitrogen-enriched dissolved organic matter in raw water and treated wastewater effluent. *Water Res.* **2013**, *47*, 2729–2741. [CrossRef]

10. Fan, Z.; Gong, S.; Xu, X.; Zhang, X.; Zhang, Y.; Yu, X. Characterization, DBPs formation, and mutagenicity of different organic matter fractions in two source waters. *Int. J. Hyg. Environ. Health* **2014**, *217*, 300–306. [CrossRef]
11. Jin, P.; Jin, X.; Bjerkelund, V.A.; Østerhus, S.W.; Wang, X.C.; Yang, L. A study on the reactivity characteristics of dissolved effluent organic matter (EfOM) from municipal wastewater treatment plant during ozonation. *Water Res.* **2016**, *88*, 643–652. [CrossRef]
12. Oh, J.H.; Jang, A. Application of chlorine dioxide (ClO_2) to reverse osmosis (RO) membrane for seawater desalination. *J. Taiwan Inst. Chem. Eng.* **2016**, *68*, 281–288. [CrossRef]
13. Ma, D.; Xia, C.; Gao, B.; Yue, Q.; Wang, Y. C-, N-DBP formation and quantification by differential spectra in MBR treated municipal wastewater exposed to chlorine and chloramine. *Chem. Eng. J.* **2016**, *291*, 55–63. [CrossRef]
14. Song, Q.; Graham, N.; Tang, Y.; Siddique, M.S.; Kimura, K.; Yu, W. The role of medium molecular weight organics on reducing disinfection by-products and fouling prevention in nanofiltration. *Water Res.* **2022**, *215*, 118263. [CrossRef] [PubMed]
15. Jiang, J.Y.; Han, J.R.; Zhang, X.R. Nonhalogenated aromatic DBPs in drinking water chlorination: A gap between NOM and halogenated aromatic DBPs. *Environ. Sci. Technol.* **2020**, *54*, 1646–1656. [CrossRef] [PubMed]
16. Zheng, L.; Song, Z.; Meng, P.; Fang, Z. Seasonal characterization and identification of dissolved organic matter (DOM) in the Pearl River, China. *Environ. Sci. Pollut. Res.* **2016**, *23*, 7462–7469. [CrossRef]
17. Deng, L.; Ngo, H.H.; Guo, W.; Zhang, H. Pre-coagulation coupled with sponge-membrane filtration for organic matter removal and membrane fouling control during drinking water treatment. *Water Res.* **2019**, *157*, 155–166. [CrossRef]
18. Zhang, B.; Xian, Q.; Gong, T.; Li, Y.; Li, A.; Feng, J. DBPs formation and genotoxicity during chlorination of pyrimidines and purines bases. *Chem. Eng. J.* **2017**, *307*, 884–890. [CrossRef]
19. Zhong, X.; Cui, C.W.; Yu, S.L. Formation of aldehydes and carboxylic acids in humic acid ozonation. *Water Air Soil Pollut.* **2017**, *228*, 1–7. [CrossRef]
20. Wen, L.; Yang, F.; Li, X. Composition of dissolved organic matter (DOM) in wastewater treatment plants influent affects the efficiency of carbon and nitrogen removal. *Sci. Total Environ.* **2023**, *857*, 159541. [CrossRef]
21. Arshad, Z.; Maqbool, T.; Shin, K.H.; Kim, S.H.; Hur, J. Using stable isotope probing and fluorescence spectroscopy to examine the roles of substrate and soluble microbial products in extracellular polymeric substance formation in activated sludge process. *Sci. Total Environ.* **2021**, *788*, 147875. [CrossRef] [PubMed]
22. Meng, Y.; Wang, M.; Guo, B.; Zhu, F.; Wang, Y.; Lu, J.; Ma, D.; Sun, Y.; Gao, B. Characterization and C-, N-disinfection byproduct formation of dissolved organic matter in MBR and anaerobic-anoxic-oxic (AAO) processes. *Chem. Eng. J.* **2017**, *315*, 243–250. [CrossRef]
23. Wang, M.; Chen, Y.G. Generation and characterization of DOM in wastewater treatment processes. *Chemosphere* **2018**, *201*, 96–109. [CrossRef] [PubMed]
24. Han, H.; Miao, H.; Zhang, Y.; Lu, M.; Huang, Z.; Ruan, W. Carbonaceous and nitrogenous disinfection byproduct precursor variation during the reversed anaerobic-anoxic-oxic process of a sewage treatment plant. *J. Environ. Sci.* **2018**, *65*, 335–346. [CrossRef] [PubMed]
25. Zhang, B.; Xian, Q.; Zhu, J.; Li, A.; Gong, T. Characterization, DBPs formation, and mutagenicity of soluble microbial products (SMPs) in wastewater under simulated stressful conditions. *Chem. Eng. J.* **2015**, *279*, 258–263. [CrossRef]
26. Jacquin, C.; Lesage, G.; Traber, J.; Pronk, W.; Heran, M. Three-dimensional excitation and emission matrix fluorescence (3DEEM) for quick and pseudo-quantitative determination of protein- and humic-like substances in full-scale membrane bioreactor (MBR). *Water Res.* **2017**, *118*, 82–92. [CrossRef]
27. Goletz, C.; Wagner, M.; Grübel, A.; Schmidt, W.; Korf, N.; Werner, P. Standardization of fluorescence excitation–emission-matrices in aquatic milieu. *Talanta* **2011**, *85*, 650–656. [CrossRef]
28. Yu, J.; Xiao, K.; Xue, W.; Shen, Y.X.; Tan, J.; Liang, S.; Wang, Y.; Huang, X. Excitation-emission matrix (EEM) fluorescence spectroscopy for characterization of organic matter in membrane bioreactors: Principles, methods and applications. *Front. Environ. Sci. Eng.* **2020**, *14*, 2095–2201. [CrossRef]
29. Wang, H.; Zhu, Y.; Hu, C.; Hu, X. Treatment of NOM fractions of reservoir sediments: Effect of UV and chlorination on formation of DBPs. *Sep. Purif. Technol.* **2015**, *154*, 228–235. [CrossRef]
30. Li, Z.; Chen, T.; Cui, F.; Xie, Y.; Xu, W. Impact of chitosan and polyacrylamide on formation of carbonaceous and nitrogenous disinfection by-products. *Chemosphere* **2017**, *178*, 26–33. [CrossRef]
31. Rodriguez, F.J.; Schlenger, P.; Garcia-Valverde, G. Monitoring changes in the structure and properties of humic substances following ozonation using UV-Vis, FTIR and (1)H NMR techniques. *Sci. Total Environ.* **2016**, *541*, 623–637. [CrossRef]
32. Liang, J.K.; Lu, Y.; Song, Z.M.; Ye, B.; Wu, Q.Y.; Hu, H.Y. Effects of chlorine dose on the composition and characteristics of chlorinated disinfection byproducts in reclaimed water. *Sci. Total Environ.* **2022**, *824*, 153739. [CrossRef] [PubMed]
33. Golea, D.M.; Upton, A.; Jarvis, P.; Moore, G.; Sutherland, S.; Parsons, S.A.; Judd, S.J. THM and HAA formation from NOM in raw and treated surface waters. *Water Res.* **2017**, *112*, 226–235. [CrossRef] [PubMed]
34. Cui, X.; Wu, B.; Liu, Y.; Ren, Q.; Ren, T.; Zhou, Y. Simultaneous and efficient removal of linear alkylbenzenesulfonate and nitrogen in a membrane biofilm reactor under low dissolved oxygen conditions. *ACS EST Eng.* **2022**, *2*, 2234–2244. [CrossRef]
35. Yin, W.; Yu, Z.; Gao, M.; Liu, Q.; Wu, B.; Ren, T.; Zhou, Y. Aeration-free greywater treatment in a self-sustaining oxygenic photobiofilm: Performance and mechanisms. *Chem. Eng. J.* **2023**, *454*, 140336. [CrossRef]

36. Xia, C.; Ma, D.; Gao, B.; Hu, X.; Yue, Q.; Meng, Y.; Kang, S.; Zhang, B.; Qi, Y. Characteristics and trihalomethane formation reactivity of dissolved organic matter in effluents from membrane bioreactors with and without filamentous bulking. *Bioresour. Technol.* **2016**, *211*, 183–189. [CrossRef] [PubMed]
37. Ma, D.; Gao, B.; Sun, S.; Wang, Y.; Yue, Q.; Li, Q. Effects of dissolved organic matter size fractions on trihalomethanes formation in MBR effluents during chlorine disinfection. *Bioresour. Technol.* **2013**, *136*, 535–541. [CrossRef]
38. Liang, S.; Zhao, Y.; Liu, C.; Song, L. Effect of solution chemistry on the fouling potential of dissolved organic matter in membrane bioreactor systems. *J. Membr. Sci.* **2008**, *310*, 503–511. [CrossRef]
39. Azami, H.; Sarrafzadeh, M.H.; Mehrnia, M.R. Soluble microbial products (SMPs) release in activated sludge systems: A review. *Iran. J. Environ. Health Sci. Eng.* **2012**, *9*, 1–10. [CrossRef]
40. Wang, Z.; Li, M.; Liao, Y.; Pan, L.; Shuang, C.; Li, J.; Zhou, Q.; Li, A. Formation of disinfection byproducts from chlorinated soluble microbial products: Effect of carbon sources in wastewater denitrification processes. *Chem. Eng. J.* **2022**, *432*, 134237. [CrossRef]
41. Shen, Y.C. Formation of nitrogenous disinfection by-products (N-DBPs) in drinking water: Emerging concerns and current issue. In *IOP Conference Series: Earth and Environmental Science*; IOP Publishing: Bristol, UK, 2015; p. 801.
42. Fan, Z.; Yang, H.; Li, S.; Yu, X. Tracking and analysis of DBP precursors' properties by fluorescence spectrometry of dissolved organic matter. *Chemosphere* **2020**, *239*, 124790. [CrossRef] [PubMed]
43. Shen, H.; Chen, X.; Zhang, D.; Chen, H.B. Generation of soluble microbial products by bio-activated carbon filter during drinking water advanced treatment and its influence on spectral characteristics. *Sci. Total Environ.* **2016**, *569*, 1289–1298. [CrossRef] [PubMed]

Disclaimer/Publisher's Note: The statements, opinions and data contained in all publications are solely those of the individual author(s) and contributor(s) and not of MDPI and/or the editor(s). MDPI and/or the editor(s) disclaim responsibility for any injury to people or property resulting from any ideas, methods, instructions or products referred to in the content.